Manuscript Details

Manuscript number	EFA_2019_1322_R1
Title	A Lifing Method based on R5 and Viscoplasticity Modelling and its Application to Turbine Rotor under Thermomechanical Loading
Article type	Research Paper

Abstract

An integrated life assessment procedure for structures operating under thermomechanical loading has been developed. The methodology uses a viscoplasticity based framework combined with the R5 life assessment code. The viscoplastic constitutive model used for the stress-strain analysis is derived from the Chaboche-Lemaitre formulation that allows to directly obtain the required parameters for the R5 assessment as stress relaxation per cycle and the elastic follow-up factor. The R5 procedure is therefore significantly simplified. The proposed life assessment procedure is demonstrated on a martensitic steel (FV566) industrial gas turbine rotor under a typical start up – shut down operation. The effect of creep-fatigue interaction at different locations within the rotor structure is assessed and the remaining life at each location is calculated. A sensitivity study is performed at half load, which shows an increase in lifetime of the rotor.

Keywords	Life Assessment; R5; Viscoplasticity; Turbine Rotors; FV566

Corresponding Author	Rossella Bonetti
Corresponding Author's Institution	Nottingham University
Order of Authors	Rossella Bonetti, Panayiotis Hadjipakkos, Yaroslav Rae, Jeremy Hughes, Wei Sun

Suggested reviewers	Christopher Truman, Haofeng Chen, Simon Wang, qiang xu, Wenchun Jiang

Submission Files Included in this PDF

File Name [File Type]

Cover letter.docx [Cover Letter]

Response to reviewers.docx [Response to Reviewers]

Highlights.docx [Highlights]

A Lifing Method based on R5 and Viscoplasticity Modelling.docx [Manuscript File]

Conflict_of_Interest.doc [Conflict of Interest]

To view all the submission files, including those not included in the PDF, click on the manuscript title on your EVISE Homepage, then click 'Download zip file'.

19-09-2019

Dear Editors-in-Chief,

We are pleased to submit an original research article entitled "*A Lifing Method based on R5 and Viscoplasticity Modelling and its Application to Turbine Rotor under Thermomechanical Loading*" by R. Bonetti, P. Hadjipakkos, Y. Rae, J. Hughes, W. Sun to be considered for publication in the *Engineering Failure Analysis.*

Thank you for your consideration.

Sincerely,

Rossella Bonetti

Responses to reviewers

Title: **A Lifing Method based on R5 and Viscoplasticity Modelling and its Application to Turbine Rotor under Thermomechanical Loading**

The authors are grateful to both the editors and reviewers for their constructive comments and suggestions, and have addressed each of these as indicated below and trust that these have resulted in a much improved manuscript.

In what follows, the authors explain how they revised (point by point) the submitted version of the paper and how they address the issues raised by the reviewer comments (*recalled in italic blue characters*). Some paragraphs and sections have been rephrased or modified as suggested by the referee. It is worth mentioning that changes and modifications, made while revising the paper, are highlighted by red characters both in this document and in the revised manuscript.

Reviewer 2

It is a good research work which industry are looking for and it is worthy being published subject to minor improvements:

1) *A brief description what about R5 about its standard procedure and information needed; then how the methodology reported in this paper speeds up its implementation.*

Section 2.2.7 has been added to explain the main differences between R5 procedure and the proposed model.

2.2.7 Advantages of the new lifing methodology

The proposed method is referred to speed up the process of stress analysis and the calculations for assessing creep-fatigue damage before crack initiation. The steps related to the cycling load histories resolution, the stress-strain curves construction and the total damage calculation are the same as in the R5 procedure.

In the R5 procedure the recourse to simplified elastic stress analysis methods is often necessary to eliminate the impracticability of inelastic computation and repeated analysis for a number of different cycles. Contrary, the viscoplastic constitutive model is considered more accurate in modelling the real mechanical response of the component under thermomechanical cyclic loadings.

For the fatigue damage calculation in the R5 procedure, the continuous cycling endurance data are presented in terms of total strain range in order to determine the number of cycles to failure. The total strain range is evaluated with a two steps procedure. Firstly, an equivalent elastic stress and strain range are calculated from the stress history for each type of cycle. Secondly, the strain range calculated elastically from the first step needs to be increased to include any enhancement due to creep and plasticity. In the proposed methodology, the strain components are a direct outputs of the FE simulation that allow the calculation of the maximum total strain range through equation (16) in the start and shut-down (as dwell contributes to creep only).

The R5 procedure for creep damage follows a complex approach that requires a description of the stress relaxation behaviour of the material. According to the material under consideration, suitable creep laws are used to define the stress relaxation

behaviour. The inelastic strain and strain rate are then obtained from stress relaxation data using the stress at the start of the dwell and the degree of the elastic follow-up parameter during the dwell period. It is usually assumed that Z is constant whereas in practice, Z changes with the stress relaxation. Contrary, in the new methodology, the creep strain as well as the stress relaxation are estimated from the FE analysis. The creep strain is the strain accumulated only over the dwell period and the start-end-of-dwell stresses are used for the calculation of stress relaxation.

2) Some description of the development of UMAT and its validation before its use.

Section 2.1.2 has been added to explain how the UMAT is developed and its validation.

2.1.2 UMAT Implementation

A UMAT subroutine is developed to numerically implement the unified viscoplasticity model through the returning mapping algorithm [13]. The purpose of the subroutine is to update the stress tensor and the other relevant quantities (inelastic strain and both hardenings) at the end of a time increment by updating the accumulated plastic strain increment Δp to which all model variables are dependent. The algorithm is composed of the elastic prediction and the inelastic correction steps.

In the elastic prediction step there is no change of the internal variables (inelastic strain, isotropic and kinematic hardening) while only the total strain is evolving. The material behaviour is thus considered fully elastic and the initial guess of the stress is determined directly by the elastic deformation. In the inelastic correction step, the stress value is corrected by allowing the internal variables to evolve while the total strain is fixed. The Newton-Raphson iteration method is used in this step to solve for the accumulated plastic strain time increment Δp by minimising the viscoplastic residue Φ [21]

$$\Phi = \Delta p - \left(\frac{f}{Z}\right)^n \tag{9}$$

The viscoplastic residue is derived from the Hooke's law and the viscoplasticity model. Equation (9) is solved with the Newton-Raphson iteration method resulting in [22]:

$$\Phi + \frac{\partial \Phi}{\partial \Delta p}\delta \Delta p + \frac{\partial \Phi}{\partial R}\delta R + \frac{\partial \Phi}{\partial \chi_i}\delta \chi_i = 0 \tag{10}$$

In this context, the symbol Δ identifies a time increment and δ is the Newton-Raphson increment.

After the evaluation of the partial derivatives in equation (10) and rearrangement, the Newton-Raphson increment of the accumulated plastic strain time increment $\delta \Delta p$ is obtained.

The accumulated plastic strain time increment Δp is finally updated by

$$\Delta p = \Delta p + \delta \Delta p \tag{11}$$

The iterative scheme ends when convergence is achieved ($|\Phi|$ less than a tolerance). The inelastic strain time increment $\Delta \varepsilon_{\mathrm{p}}$ is determined from equations (1) and (2). The stress increment is finally given as

$$\boldsymbol{\Delta\sigma} = E(\Delta\boldsymbol{\varepsilon} - \boldsymbol{\Delta\varepsilon_p}) \quad (12)$$

Extensive validation of the model have been performed and its capability to simulate hysteresis loops from experimental data has been checked. Isothermal hold-time low cycle fatigue tests have been conducted in the temperature range from 400 to 600°C for FV566 [13, 21] and on P91-P92 steels [23-25]. The stress-strain material response from the model and the experiments have been compared and a good agreement has been found [21]. Particularly, an example with stress relaxation is shown in Figure 2 for P92 tested at 600°C and ±0.5% strain amplitude. The capability of the unified viscoplasticity model has shown to give accurate prediction [25].

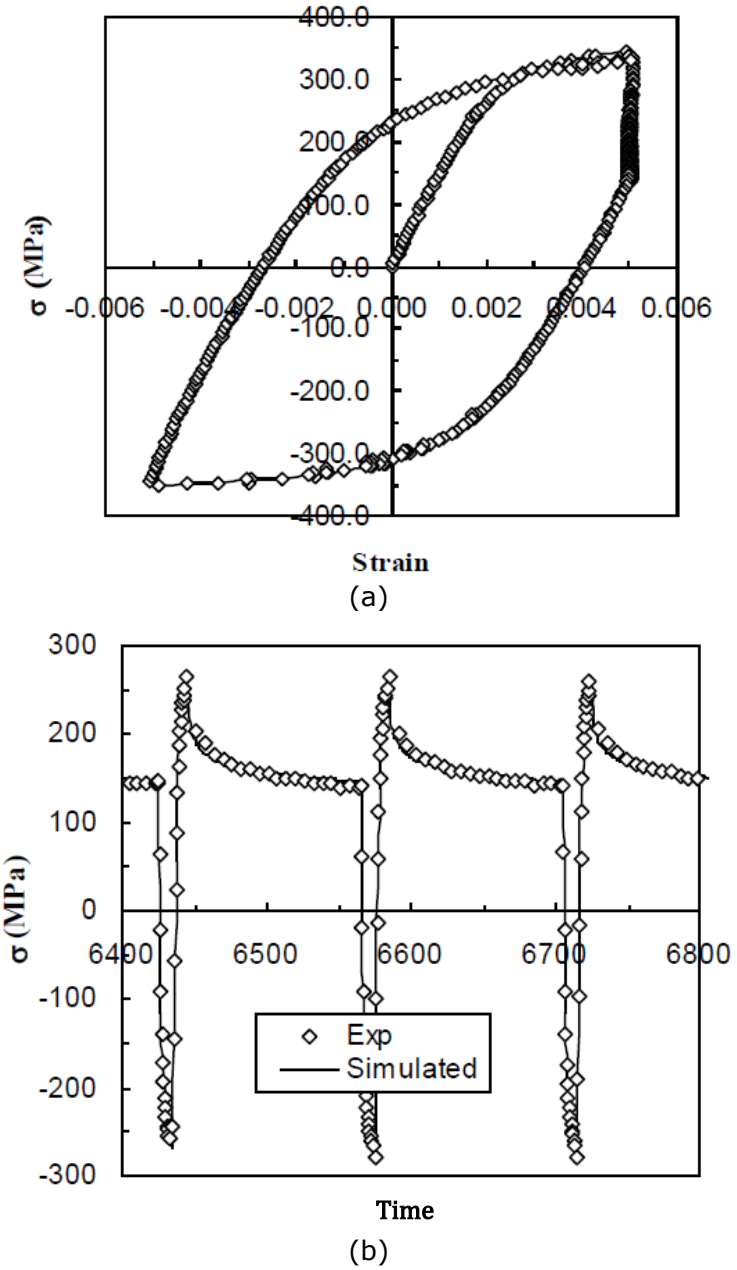

Figure 2: Results for P92 at 600°C and ±0.5% strain amplitude (a) experimental stress-strain hysteresis loop (b) experimental and model stress-time curves comparison [25]

3) Describe the method used to calculate the Failure (hr) in table 4; the accuracy for different damage is not consistent which should be corrected.

In section 4.3 a short paragraph has been added to explain how the failure in hours has been derived from the cycle to failure and the damage values have been corrected.

In the text it is reported as below:

Table 4: Summary of the calculated damage values and total life estimations

Location	Fatigue damage/cycle, D_f	Creep damage/cycle, D_c	Total damage, D	Cycles to failure	Failure (hr)
		Original Load (3,000rpm)			
Loc1 (Hot region)	0.00012	0.000075	0.000195	5,128	123,077
Loc2 (Cold region)	0.000093	0.000012	0.000105	9,524	228,571
		Half Load (1,500rpm)			
Loc1 (Hot region)	0.000035	0.000073	0.000108	9,259	222,222
Loc2 (Cold region)	0.000027	0.000011	0.000038	26,316	631,579

The failure in hours is calculated from the cycles to failure considering that the duration of one cycle is 24 hours as stated in section 3.2.

- An integrated life assessment framework for structures under thermomechanical loadings is proposed.
- The framework is based on R5 and viscoplasticity modelling.
- The procedure is implemented on an industrial gas turbine.

A Lifing Method based on R5 and Viscoplasticity Modelling and its Application to Turbine Rotor under Thermomechanical Loading

R. Bonetti[a,*], P. Hadjipakkos[a], Y. Rae[a], J. Hughes[b], W. Sun[a]

[a] *Department of Mechanical, Materials and Manufacturing Engineering, University of Nottingham, Nottingham, NG7 2RD, UK*

[b] *RWE Generation (UK), Windmill Hill Business Park, Whitehill Way, Swindon, SN5 6PB, UK*

ABSTRACT

An integrated life assessment procedure for structures operating under thermomechanical loading has been developed. The methodology uses a viscoplasticity based framework combined with the R5 life assessment code. The viscoplastic constitutive model used for the stress-strain analysis is derived from the Chaboche-Lemaitre formulation that allows to directly obtain the required parameters for the R5 assessment as stress relaxation per cycle and the elastic follow-up factor. The R5 procedure is therefore significantly simplified. The proposed life assessment procedure is demonstrated on a martensitic steel (FV566) industrial gas turbine rotor under a typical start up – shut down operation. The effect of creep-fatigue interaction at different locations within the rotor structure is assessed and the remaining life at each location is calculated. A sensitivity study is performed at half load, which shows an increase in lifetime of the rotor.

Keywords: Life Assessment; R5; Viscoplasticity; Turbine Rotors; FV566

** Corresponding author: Rossella.Bonetti@nottingham.ac.uk*

1. Introduction

The drive towards sustainability has led modern industrial plants, typically in the petrochemical and in the energy industries, to operate under extreme temperatures and pressures as well as to experience more frequent start-up and shut-down operations. Future designs of ultra-supercritical power plants aim to operate at temperatures up to 760°C and pressures of 350 bar [1]. Furthermore, the changing nature of the electricity market, along with the significant addition of renewables in the grid, has forced power plants to become more 'flexible' in their operations, with a transition from base-load to intermittent modes of operation. These extreme operating conditions subject plant to time-dependent creep deformation due to elevated temperatures and pressures, as well as Low Cycle Fatigue (LCF) due to more frequent mechanical and temperature cyclic loadings. The combination of these two modes of failure (known as creep-fatigue interaction) can significantly reduce the safe, in-service life of components. The occurrence of LCF behaviour, especially on structures operating inside the creep regime can significantly accelerate their long term deterioration and encourage crack nucleation and propagation, resulting in an early failure. Dundas also suggested that over 62% of the total damage costs of gas turbines involve cycle cooling, fatigue, creep and surge related failures [2]. Therefore, the failure of components due to the combined effects of creep and fatigue becomes a critical issue and of considerable interest to investigators for both design and in-service life assessment [3, 4]. Knowledge concerning the long-term behaviour of materials under such extreme conditions is required for the appropriate fail-safe design decisions. Accurate deformation, damage evolution and rupture life prediction information could also result in economic and effective maintenance by appropriately scheduling inspection, maintenance and repair time periods, mitigating the risk of unexpected shut downs.

Great efforts have been made to investigate the response of materials subjected to cyclic loading conditions. Most of the early material models were based on the Coffin-Manson and Basquin laws which describe the fatigue (elastic-plastic) behaviour of materials [5]. These models have been commonly used in industry due to their simplicity and accuracy in describing the material deformation at low temperature [6, 7]. Later, many damage models were developed to predict the life of structures under variable temperature and loading conditions [8-10]. At high temperatures the materials exhibit also creep (viscous) behaviour in the plastic region [11]. Thus, using a simple elastic-plastic model to reproduce the non-linear viscoplastic response of materials can result in poor predictions, especially during high temperature, cyclic loading. Instead, viscoplasticity models are needed for analysing creep and fatigue behaviour.

The Chaboche constitutive viscoplastic model is commonly employed for this purpose. Chaboche proposed a phenomenological based unified model which combined isotropic and kinematic hardening variables in a viscoplasticity-flow rule, taking into account cyclic hardening/softening and the Bauschinger effect [12]. The model has been used extensively by many authors to study the responses of materials under creep-fatigue conditions and shows a good agreement with the experimental results [13-15].

For the purpose of life assessment, creep-fatigue life prediction approaches generally involve the calculation of creep damage and fatigue damage separately. The rupture time or the number of cycles to failure can be then evaluated by combining both damage values using a linear interaction rule. A common approach to calculate creep damage is by using a time-fraction rule. This approach was also adopted in the life assessment procedure of the American Society of Mechanical Engineers (ASME) as well as in the French RCC-MR Codes [16, 17]. However, it was observed that the predicted results when the time-fraction rule was used differed in each code. The variation in the results is due to several detailed differences between the codes regarding the safety factors on creep rupture curves and the interaction rules used to combine the creep and the fatigue damage. Instead of using a time-fraction rule, an alternative approach is to consider the ductility exhaustion method more capable of accurately predicting the material life. The ductility exhaustion approach has been adopted and further developed in the British R5 assessment procedure [18, 19]. The R5 life assessment procedure is currently used to assess plant integrity within the UK power generation industry and it involves numerous steps for the determination of required parameters, such as the stress relaxation per cycle and the elastic follow-up factor.

The main objective of the present investigation is to develop a clear guideline, a framework to be used for the life assessment of structures subjected to thermomechanical loadings. This involves the possibility of linking the Chaboche constitutive viscoplasticity model with the R5 assessment procedure with the aim to allow more accurate life estimations and to simply the lifing assessment procedure. This integrated lifing model is applied to an industrial gas turbine rotor made from FV566 martensitic steel, a common material used in high temperature applications [20].
The effectiveness of the new lifing procedure is demonstrated.

2. Development of the New Lifing Model

The constitutive Chaboche viscoplasticity model is implemented in the ABAQUS FE software using the user-defined sub-routine UMAT to perform the stress analysis of the turbine rotor. The model has the ability to describe the plastic deformation as well as the viscous behaviour of the material, so that accurate stress-strain predictions can be

obtained. Additionally, important parameters required for the R5 life assessment procedure such as the stress relaxation per cycle and the elastic-follow up factor can be obtained directly from the model, avoiding several complicated steps of the R5 procedure. A flowchart of the integrated life assessment procedure developed is shown in Figure 1.

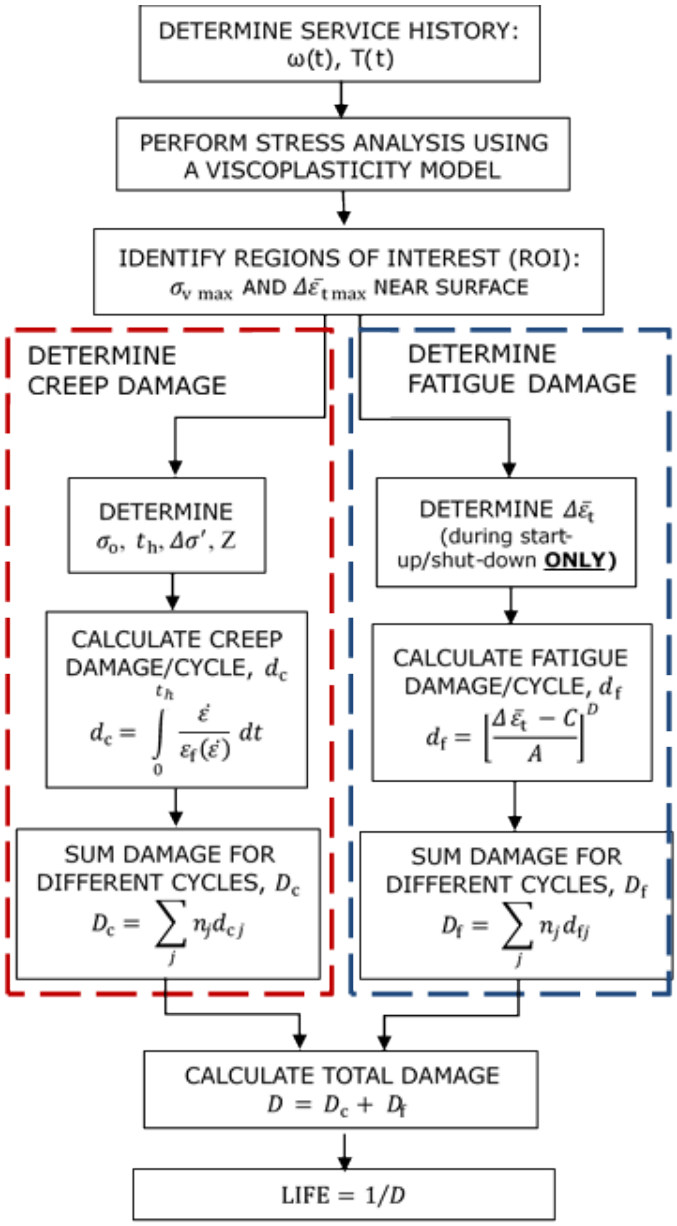

Figure 1: The process flowchart of the integrated lifing model developed

2.1 Unified Viscoplasticity Modelling

2.1.1 Constitutive equations

In the Chaboche unified constitutive model, the rate-dependent inelastic strain is used to represent both creep (viscous) and plastic strains [12]. This inelastic strain rate, $\dot{\boldsymbol{\varepsilon}}_p$ is defined by the following equation:

$$\dot{\boldsymbol{\varepsilon}}_p = \left\langle \frac{f}{Z} \right\rangle^n sgn(\boldsymbol{\sigma} - \boldsymbol{\chi}) \tag{1}$$

where f is a yield function which determines the elastic limit, n and Z are material parameters which describe the evolution of viscous stress, $\boldsymbol{\sigma}$ is the total stress tensor and $\boldsymbol{\chi}$, the kinematic hardening tensor, also known as back stress, responsible for the cyclic loading and changes due to inelastic loading. The accumulated viscoplastic strain rate is defined by:

$$\dot{p} = |\dot{\boldsymbol{\varepsilon}}_{\mathbf{p}}| \tag{2}$$

The yield function for the model can be expressed as:

$$f = |\boldsymbol{\sigma} - \boldsymbol{\chi}| - R - k \tag{3}$$

where R is the isotropic hardening parameter, also known as drag stress. The elastic domain is defined by $f \leq 0$ and the inelastic domain is defined by $f > 0$. The evolution of R and $\boldsymbol{\chi}_i$ values are controlled by the following equations. The isotropic hardening, drag stress evolution $\dot{R}$ is represented by:

$$\dot{R} = b(Q - R)\dot{p} \tag{4}$$

where b determines how quickly the drag stress is stabilised, Q is a stabilised value of drag stress after a specific accumulation of plastic strain and $\dot{p}$ is the accumulated plastic strain rate. The kinematic hardening, back stress evolution, $\dot{\boldsymbol{\chi}}$ is represented by:

$$\dot{\boldsymbol{\chi}}_{\boldsymbol{\iota}} = C_i(a_i\dot{\boldsymbol{\varepsilon}}_{\mathbf{p}} - \boldsymbol{\chi}_{\boldsymbol{\iota}}\dot{p}) \tag{5}$$

$$\boldsymbol{\chi} = \sum_{\iota}^{M} \boldsymbol{\chi}_{\boldsymbol{\iota}} \tag{6}$$

where a_i and $C_i\ (i = 1, 2)$ are temperature-dependent material constants, similar to Q and b. The viscous stress can be expressed as:

$$\sigma_{\mathrm{v}} = Z\dot{p}^{1/n} \tag{7}$$

and finally the total stress can be decomposed as:

$$\boldsymbol{\sigma} = \boldsymbol{\chi} + (R + k + \sigma_{\mathrm{v}})\, sgn(\boldsymbol{\sigma} - \boldsymbol{\chi}) = E(\boldsymbol{\varepsilon} - \boldsymbol{\varepsilon}_{\mathbf{p}}) \tag{8}$$

The constants of the viscoplasticity model are calibrated from isothermal fatigue and stress relaxation experiments on FV566 martensitic steel [21].

2.1.2 UMAT Implementation

A UMAT subroutine is developed to numerically implement the unified viscoplasticity model through the returning mapping algorithm [13]. The purpose of the subroutine is to update the stress tensor and the other relevant quantities (inelastic strain and both hardenings) at the end of a time increment by updating the accumulated plastic strain increment Δp to which all model variables are dependent. The algorithm is composed of the elastic prediction and the inelastic correction steps.

In the elastic prediction step there is no change of the internal variables (inelastic strain, isotropic and kinematic hardening) while only the total strain is evolving. The material

behaviour is thus considered fully elastic and the initial guess of the stress is determined directly by the elastic deformation. In the inelastic correction step, the stress value is corrected by allowing the internal variables to evolve while the total strain is fixed. The Newton-Raphson iteration method is used in this step to solve for the accumulated plastic strain time increment Δp by minimising the viscoplastic residue Φ [21]

$$\Phi = \Delta p - \left(\frac{f}{Z}\right)^n \tag{9}$$

The viscoplastic residue is derived from the Hooke's law and the viscoplasticity model. Equation (9) is solved with the Newton-Raphson iteration method resulting in [22]:

$$\Phi + \frac{\partial \Phi}{\partial \Delta p}\delta \Delta p + \frac{\partial \Phi}{\partial R}\delta R + \frac{\partial \Phi}{\partial \chi_i}\delta \chi_i = 0 \tag{10}$$

In this context, the symbol Δ identifies a time increment and δ is the Newton-Raphson increment.

After the evaluation of the partial derivatives in equation (10) and rearrangement, the Newton-Raphson increment of the accumulated plastic strain time increment $\delta \Delta p$ is obtained.

The accumulated plastic strain time increment Δp is finally updated by

$$\Delta p = \Delta p + \delta \Delta p \tag{11}$$

The iterative scheme ends when convergence is achieved ($|\Phi|$ less than a tolerance). The inelastic strain time increment $\Delta \varepsilon_{\mathrm{p}}$ is determined from equations (1) and (2). The stress increment is finally given as

$$\boldsymbol{\Delta \sigma} = E(\Delta \boldsymbol{\varepsilon} - \boldsymbol{\Delta \varepsilon_{\mathrm{p}}}) \tag{12}$$

Extensive validation of the model have been performed and its capability to simulate hysteresis loops from experimental data has been checked. Isothermal hold-time low cycle fatigue tests have been conducted in the temperature range from 400 to 600°C for FV566 [13, 21] and on P91-P92 steels [23-25]. The stress-strain material response from the model and the experiments have been compared and a good agreement has been found [21]. Particularly, an example with stress relaxation is shown in Figure 2 for P92 tested at 600°C and ±0.5% strain amplitude. The capability of the unified viscoplasticity model has shown to give accurate prediction [25].

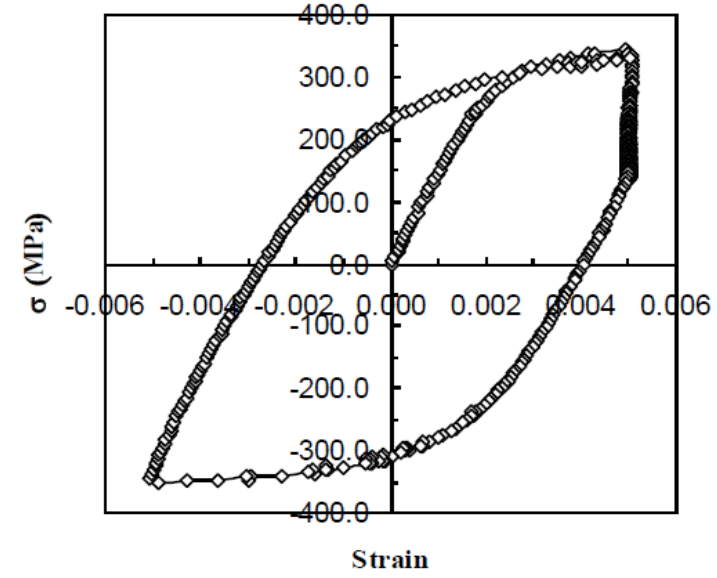

(a)

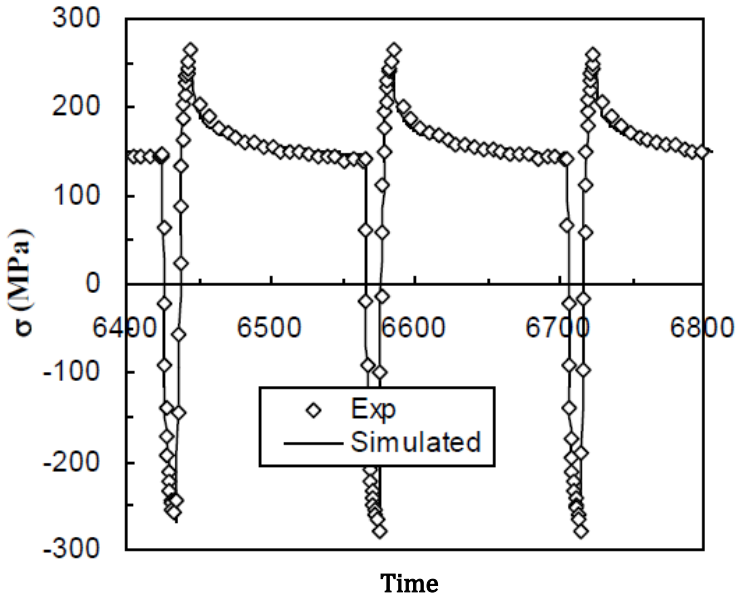

(b)

Figure 2: Results for P92 at 600°C and ±0.5% strain amplitude (a) experimental stress-strain hysteresis loop (b) experimental and model stress-time curves comparison [25]

2.2 Integrated Life Assessment Procedure

Linking the viscoplasticity model with R5 code, a novel integrated life assessment procedure is developed. The procedure consists of 6 steps which are described in the following section.

2.2.1 Resolution of the load history into different service cycles

The complete cyclic load history experienced by the component needs to be determined. A service cycle is defined as a repeated sequence of operation, where the initial and final loading and temperature states are the same. In most cases, raw data includes fluctuations which lead to the formation of small cycles inside a larger cycle. In this case, for simplicity, the small cycles can be superposed and form a unique cycle with a dwell. In

cases where the cycles are of different loading magnitudes and also involve an associated dwell period, they have to be grouped accordingly to different cycle types. The actual load history can be then simplified and divided into distinct cyclic events or service cycles, each involving an associated cyclic load, a constant load during the dwell period and the associated temperature of the dwell. This resolves the actual load history in a well-defined number of different service cycles. A graphical representation of the procedure can be seen in Figure 3.

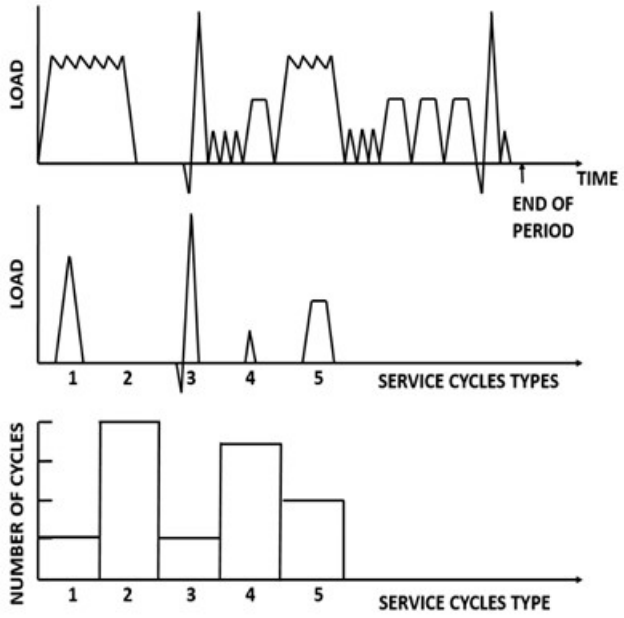

Figure 3: Resolution of loading history into different service cycles types

2.2.2 Stress analysis using a viscoplasticity material model

This step requires stress analysis to be performed on each different service cycle. The stress analysis should model the overall mechanical responses of the component. During the stress analysis, the main regions of interest have to be identified. These include:

i) locations where maximum von Mises stresses, usually near the surface of the geometry;
ii) locations where the maximum total equivalent strain range occurs during the cycle, again usually near the surface and
iii) the hottest locations where creep is significant.

These locations are considered to be the most damaging positions in the rotor, which are most likely to experience crack initiation eventually leading to failure. The accuracy of any stress analysis is always dependent on the ability of the material model and the associated material properties used to reproduce the cyclic responses of the material.

2.2.3 Construction of cyclic deformation loops

Results from the stress analysis can provide the necessary data to construct the cyclic deformation stress-strain loops for each of the different locations selected from the previous step and also for each of the different service cycles. The expected loop should not be closed but should include an increment of strain which is accumulated at each cycle. This accumulation of strain can be an effect of forward creep deformation due to the primary load or elastic follow-up. A typical cyclic deformation loop can be seen in Figure 4. From each of the stress-stain loops constructed, important information can be extracted that will be used in later steps of the life assessment. These include: i) the total cyclic strain range, $\Delta\varepsilon_{\mathrm{t}}$ ii) the position of the dwell which can be characterized from the stress at the start of the dwell σ_{o} and the duration of the dwell t_{h} allowing the user to determine the

stress relaxation $\Delta\sigma'$ due to the dwell for the cycle and iii) the elastic follow-up parameter, Z .

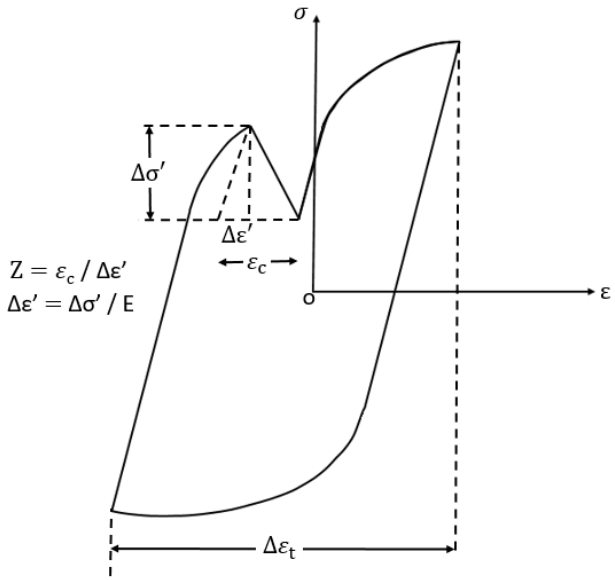

Figure 4: Schematic of the cyclic deformation loop

2.2.4 Fatigue damage calculation

The fatigue damage associated with each service cycle can be evaluated using the endurance curve approach. This approach requires a complete cyclic endurance data set of the material tested. These data can be usually obtained from simple specimen testing under uniaxial tensile control. The endurance curve can be expressed as:

$$N_f = \left[\frac{A}{\Delta\bar{\varepsilon}_{t\,max} - C}\right]^D \tag{13}$$

where A, C and D are material constants obtained by fitting, N_f is the number of cycles to failure and $\Delta\bar{\varepsilon}_{t\,max}$ is the maximum equivalent total strain range during the start-up and shut-down operations of the cycle, excluding the dwell region as it is assumed that dwell contributes to creep damage only.

First, it is necessary to calculate the change of each strain component ε_{ij} between time t and t' inside the service cycle. For example the strain range in the 11-direction is given by:

$$\varepsilon_{11}(t, t') = \varepsilon_{11}(t) - \varepsilon_{11}(t') \tag{14}$$

and more generally,

$$\varepsilon_{ij}(t, t') = \varepsilon_{ij}(t) - \varepsilon_{ij}(t') \qquad \forall\ i, j \tag{15}$$

The equivalent strain range, $\bar{\varepsilon}(t, t')$ can be obtained from the components $\varepsilon_{ij}(t, t')$ by the following formula:

$$\bar{\varepsilon}(t,t') = \frac{\sqrt{2}}{3}\left\{\left[\varepsilon_{11}(t,t') - \varepsilon_{22}(t,t')\right]^2 + \left[\varepsilon_{22}(t,t') - \varepsilon_{33}(t,t')\right]^2 + \left[\varepsilon_{33}(t,t') - \varepsilon_{11}(t,t')\right]^2 + \left[\varepsilon_{12}^2(t,t') + \varepsilon_{23}^2(t,t') + \varepsilon_{31}^2(t,t')\right]\right\}^{1/2} \quad (16)$$

The strain range obtained with the highest value is considered to be the maximum equivalent total strain range value, $\Delta\bar{\varepsilon}_{\mathrm{t\,max}}$, in the cycle. This should be then converted into a percentage and used in the endurance equation to calculate the number of cycles to failure, N_{f}. The fatigue damage for each cycle d_{f} is defined as $1/N_{\mathrm{f}}$, the inverse of the number of cycles to failure.

2.2.5 Creep damage calculation

The creep damage associated with each service cycle can be evaluated using the ductility exhaustion approach. The creep damage per cycle, d_{c}, can be obtained by dividing the inelastic creep strain during the dwell period, t_{h}, by an appropriate ductility value. The ductility exhaustion approach involves the inelastic strain rate, the elastic follow-up as well as the dwell period and can be evaluated by:

$$d_c = \int_0^{t_h} \frac{\dot{\varepsilon}_c}{\varepsilon_{\mathrm{f}}(\dot{\varepsilon}_c)}\, dt \quad (17)$$

where $\dot{\varepsilon}_c$ is the instantaneous inelastic strain rate during the dwell period and $\varepsilon_{\mathrm{f}}(\dot{\varepsilon})$ is the corresponding creep ductility. During the steady-state period of operation, an inelastic strain is formed by the conversion of the elastic strain when the stress relaxation occurs in conjunction with the forward creep deformation from the primary load. The effect of the combination of the two processes can be defined as the elastic follow-up parameter, Z, and the increment of the inelastic strain for the cycle can be obtained by:

$$\varepsilon_c = -\frac{Z}{E}\Delta\sigma' \quad (18)$$

where E is the young's modulus of the material and $\Delta\sigma'$ is the stress relaxation during the dwell period, t_{h}. Hence, the instantaneous deformation can be expressed as:

$$\dot{\varepsilon}_c = -\frac{Z}{E}\frac{\Delta\sigma'}{dt} \quad (19)$$

The creep damage can be then determined by two methods. The first method should be used when the dwell is in the tensile part of the cycle. By assuming that the engineering strain, ε_{f}, is independent of the strain rate and equal to the lower shelf ductility ε_L of the material, equation (17) may be simplified to:

$$d_c = \frac{Z}{E}\frac{\Delta\sigma'}{\varepsilon_L} \quad (20)$$

Similarly, if the dwell is in the compressive part of the cycle, the upper shelf ductility of the material, ε_U, should be used and the creep damage of the cycle can be determined by:

$$d_c = \frac{Z}{E}\frac{\Delta\sigma'}{\varepsilon_U} \tag{21}$$

2.2.6 Total damage calculation

The total damage, D, is predicted to accumulate during the lifetime of the component and can be calculated from the fatigue and creep damage of each service cycle as outlined in the previous steps. The total damage, D, is defined as the linear sum of a fatigue component D_{f}, and a creep component, D_{c}. It is assumed that failure occurs when D reaches 1 as shown in Figure 5.

$$D = D_{\mathrm{f}} + D_{\mathrm{c}} \tag{22}$$

where,

$$D_{\mathrm{f}} = \sum_j n_j / N_{\mathrm{f}j} = \sum_j n_j d_{\mathrm{f}j} \tag{23}$$

and,

$$D_{\mathrm{c}} = \sum_j n_j d_{cj} \tag{24}$$

where n_j is the number of cycles of type j and $N_{\mathrm{f}j}$, $d_{\mathrm{f}j}$ and d_{cj} is the value of N_{f}, d_{f} and d_{c} corresponding to that cycle type.

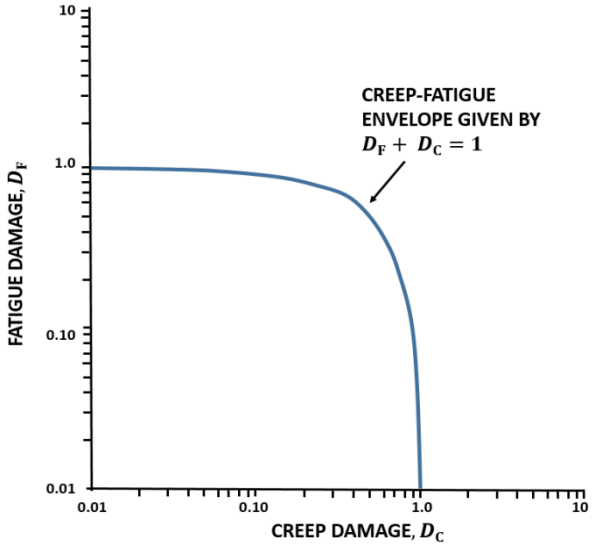

Figure 5: The damage diagram

2.2.7 Advantages of the new lifing methodology

The proposed method is referred to speed up the process of stress analysis and the calculations for assessing creep-fatigue damage before crack initiation. The steps related to the cycling load histories resolution, the stress-strain curves construction and the total damage calculation are the same as in the R5 procedure.

In the R5 procedure the recourse to simplified elastic stress analysis methods is often necessary to eliminate the impracticability of inelastic computation and repeated analysis for a number of different cycles. Contrary, the viscoplastic constitutive model is considered

more accurate in modelling the real mechanical response of the component under thermomechanical cyclic loadings.

For the fatigue damage calculation in the R5 procedure, the continuous cycling endurance data are presented in terms of total strain range in order to determine the number of cycles to failure. The total strain range is evaluated with a two steps procedure. Firstly, an equivalent elastic stress and strain range are calculated from the stress history for each type of cycle. Secondly, the strain range calculated elastically from the first step needs to be increased to include any enhancement due to creep and plasticity. In the proposed methodology, the strain components are a direct outputs of the FE simulation that allow the calculation of the maximum total strain range through equation (16) in the start and shut-down (as dwell contributes to creep only).

The R5 procedure for creep damage follows a complex approach that requires a description of the stress relaxation behaviour of the material. According to the material under consideration, suitable creep laws are used to define the stress relaxation behaviour. The inelastic strain and strain rate are then obtained from stress relaxation data using the stress at the start of the dwell and the degree of the elastic follow-up parameter during the dwell period. It is usually assumed that Z is constant whereas in practice, Z changes with the stress relaxation. Contrary, in the new methodology, the creep strain as well as the stress relaxation are estimated from the FE analysis. The creep strain is the strain accumulated only over the dwell period and the start-end-of-dwell stresses are used for the calculation of stress relaxation.

3. Application of the Lifing Model to An Industrial Gas Turbine Rotor

The developed life assessment procedure is demonstrated in the analysis of an industrial gas turbine rotor operating under realistic load conditions. The rotor assessed is taken from a 300MW gas turbine used in a combined-cycle power plant. The rotor itself is made from FV566 martensitic steel and comprises 3 major sections: a 4-stage low pressure turbine (LPT), a single-stage high pressure turbine (HPT) and a 23-stage compressor. The full-geometry of the turbine rotor can be seen in Figure 6.

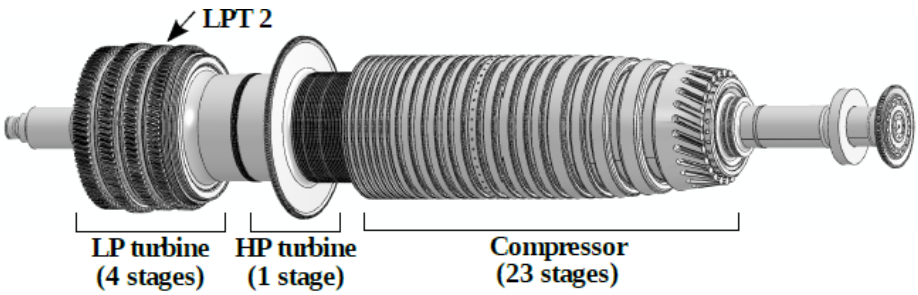

Figure 6: Full geometry of gas turbine rotor

The rotor is simulated in ABAQUS FE software using the constitutive Chaboche elasto-viscoplasticity model implemented using UMAT sub-routine. Taking advantage of the radial symmetry in the geometry of the rotor, the model is built as a 2D axisymmetric problem. The material properties used including all material constants required for UMAT subroutine are obtained from Rae et al [21] (Table 2).

The simulation consists of two steps:

i) Heat transfer step to determine the temperature distribution during the loading.
ii) Thermo-mechanical stress analysis performed using temperature data from step 1 together with mechanical loads.

3.1 FV566 Steel and Viscoplastic Model Properties

FV566 (X12CrNiMo12-3) is a type of tempered martensitic steel often used in high temperature industrial applications for its high creep and thermal-fatigue strength. The specific chemical composition of FV566 is given in Table 1 [21]. The base FV566 microstructure shows prior austenitic grains (PAGs) that contain one or more packets. Inside the packets, blocks of laths and subgrain regions are identified. An EBSD image of FV566 base material is shown in Figure 7 [26].

Table 1: FV566 martensitic steel chemical composition [21]

Element	*C*	*Si*	*Mn*	*Cr*	*Mo*	*Ni*	*V*	*S*	*Fe*
Weight (%)	0.16	0.038	0.668	11.9	1.68	2.52	0.298	0.0006	Remainder

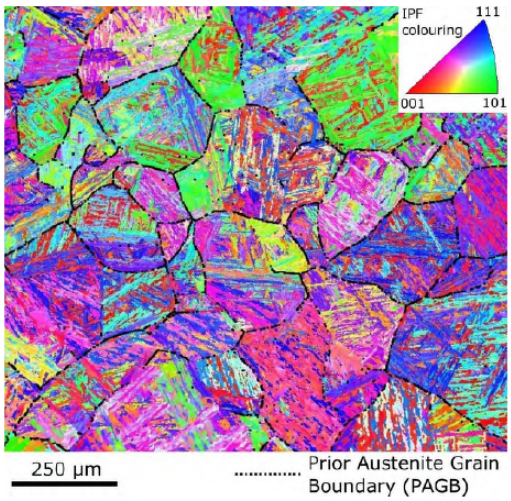

Figure 7: EBSD map of FV566 base material microstructure [26]

The viscoplastic model material properties are determined through a 2 steps process. Initial guess of material parameters are extracted from isothermal uniaxial strain-controlled saw-tooth (SWT) and dwell-type (DWT) tests. Following, an optimisation procedure is performed with Matlab routine for model validation. The SWT and DWT waveforms together with the specimen geometry used for material parameters identification are depicted in Figure 8 [21].

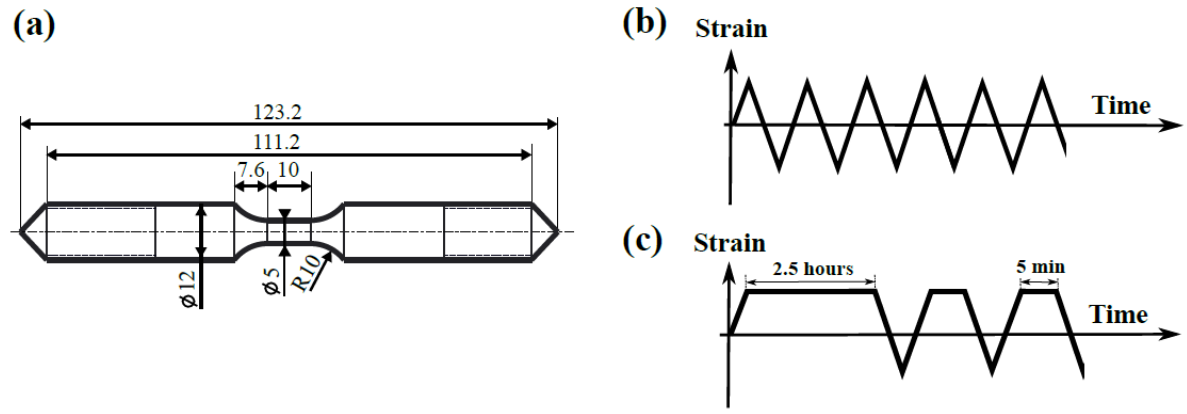

Figure 8: (a) dimensions and geometry of the specimen (measures in mm). Waveforms used for (b) fatigue saw-tooth and (c) creep-fatigue dwell type tests

From experimental tests and the optimisation procedure, the Chaboche material model parameters are found to evolve linearly with the temperature. Their relationship is shown in Table 2 [21].

Table 2: Material parameters evolution with temperature [21]

Mechanical feature	*Symbol*	*Unit*	*Fitting equation*
Elasticity	E	GPa	-0.3726*T*+322.36
	k	MPa	-1.07*T*+806.98
Non-linear viscosity	Z	MPa	235.48*T*-93419
	n	-	-0.02375*T*+15.322
Kinematic hardening	C_1	-	-0.06525*T*+52.352
	a_1	MPa	-6.1245*T*+3989.3
Isotropic hardening	b	-	-0.00505*T*+4.945
	Q	MPa	-0.1678*T*-9.0067

3.2 Finite Element Model

The rotor FE model geometry and mesh are shown in Figure 9. Finer mesh is used near the surface of the rotor to accurately reproduce heat transfer effects on temperature and stress/strains.

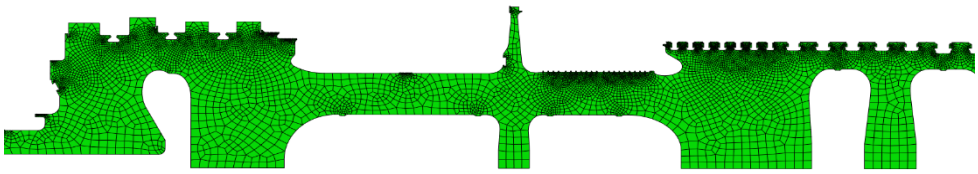

Figure 9: Finite element mesh from a section of the gas turbine rotor

The simulation is taken through 10-cycles of operation. Each cycle represents a typical day (24 hours) for a peaking power plant. This includes a start-up, a dwell period at full load (3000rpm), a shut-down and finally a dwell period at rest. A load sensitivity study is performed to estimate the variation on the final lifetime prediction with a second simulation at half load. The loading pattern showing the variation of the rotational speed and temperature during the cycles for the base case simulation is shown in Figure 10.

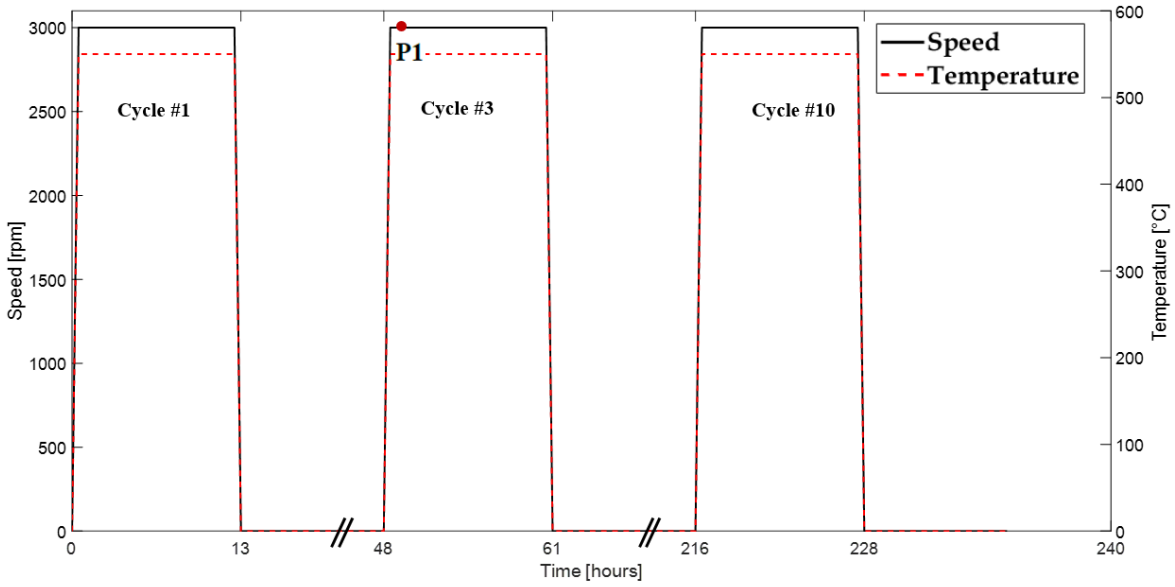

Figure 10: A typical loading patter experienced in a peaking power plant

3.3 Thermo-Mechanical Loading

The temperature distribution along the turbine rotor is non-uniform. During its operation, ambient air is drawn into the compressor inlet which keeps the rotor temperature relatively low in this region. The inlet air temperature is conservatively assumed to be at 11°C. As the air is compressed, its temperature increases, consecutively increasing the rotor temperature, as the surface of the rotor is exposed to the hot air. At the compressor outlet, the air is at its most compressed state which results in high temperatures in the region. The surface of the rotor at the compressor outlet reaches a maximum temperature of about 550°C. The rotor temperature in the HPT region continues to be kept high, as it is exposed to hot gases from the combustion chamber. The temperature subsequently drops in the LPT due to forced cooling from the cooling holes. The temperature distribution of the surface of the turbine rotor during the dwell period at full load can be seen in Figure 11. Similar thermal profiles for different periods of the rotor operation (start-up and shut-down) are applied to the surface of the rotor in order to set the thermal boundary conditions of the model.

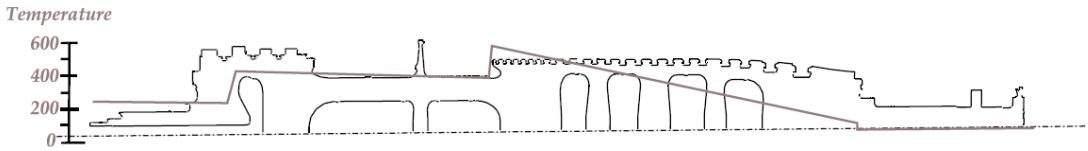

Figure 11: Surface temperature distribution along the length of the rotor at full load

The mechanical load on the turbine rotor is composed of the centrifugal forces generated due to the mass of the rotor and the contact pressure at the blade root locations. Both parameters vary with time as they both depend on the rotational speed. The rotational speed is applied directly within ABAQUS using a material density of 7750 kg/m3. Additional pressure loads are also applied to the blade root locations. These are calculated using the mass and the centre of gravity of each blade.

4. Results and Discussion

4.1 Temperature and Stress Analysis

The results of the simulation described in the previous section are analysed to identify the regions of interest within the rotor structure.

One important time point in the loading cycle (P1, Figure 10) is considered for the analysis in which the contribution of thermal stresses is expected to be high after the start-up. P1 is located at the start of the dwell (Figure 10) at the 3rd cycle. Figure 12 shows the temperature and von Mises stress response of the rotor at P1 after 3 cycles.

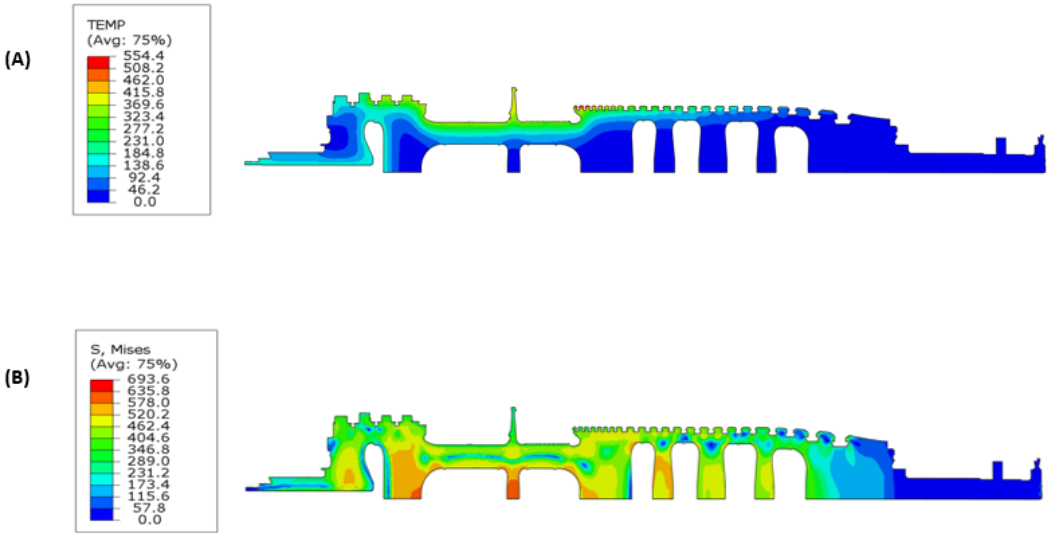

Figure 12: Temperature and von Mises stress contour for the 3rd cycle at P1

At the start of the dwell at point P1, a non-uniform temperature distribution is observed (Figure 12A). The inside of the rotor still remains relatively cool although the temperature is already at the peak value of the dwell. More time is required for the heat transfer due to conduction to occur and which gradually moves the heat to the core of the rotor. The highest temperatures are observed in the final stage of the compressor as well as in the HPT region. The first stages of the compressor do not show any significant rise in temperature as they are continuously cooled from the cold air drawn inside. The corresponding von Mises contour plot at time point P1 shows a significant variation in the thermal stresses distribution, particularly in the central areas of the rotor (Figure 12B). The maximum von Mises stress is located at the blade insertion groove of the second compressor stage mainly because of the large blade mass and the rotational speed. The geometric discontinuities in these regions act as stress concentrators. The main area where high stress variation occur is at the transition between HPT and LPT.

The second simulation at half load shows similar stress distributions as the full load model with identical temperature predictions.

4.2 Regions of Interest

In Figure 13, two surface locations are presented for the purpose of life assessment. These include: i) a point of high stress in a hot region of the turbine rotor (Loc1) and ii) a point of high stress in a cold region of the rotor (Loc2).

(Loc1) is located at the first stage of the LPT whereas (Loc2) is located at the first stage of the compressor.

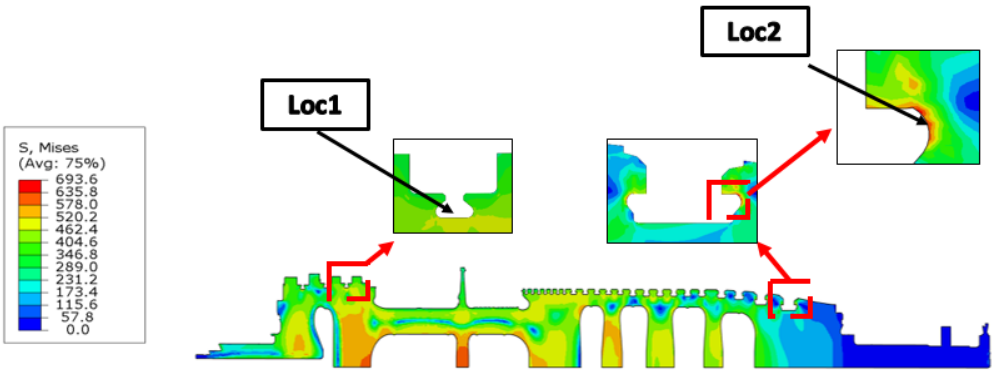

Figure 13: Life assessment locations based on von Mises stress

The highest stresses at both locations are observed during the end of the start-up operation, just when the dwell period starts. These high stresses are induced mainly because of the high pressures generated when the rotor reaches its maximum rotational speed (3,000rpm) and also due to the addition of thermal stresses which are induced from the large temperature gradients during the start-up operation.

The highest von Mises stresses observed at (Loc1) and (Loc2) are 355MPa and 440MPa respectively. During the dwell period, the magnitude of the stresses at the entire surface of the rotor shows a decreasing trend by time due to stress relaxation behavior. The dwell period during the 3rd cycle causes the stress at (Loc1) to relax by 115MPa whereas at (Loc2) by only 21MPa. These results would have a significant impact on the final life prediction, as it can be observed from equations (20, 21). The stress relaxation behaviour for (Loc1) and (Loc2) can be seen in Figure 14.

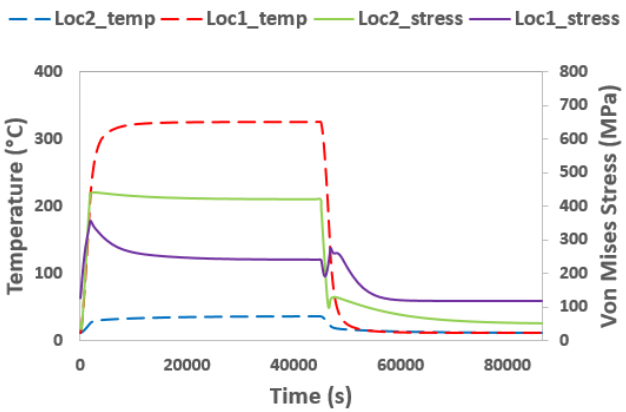

Figure 14: Evolutions of von Mises stress for Loc1-3

4.3 Damage and Life Assessment

The life assessment procedure described in Section 2.2 is conducted for both locations identified within the rotor structure (Loc1, Loc2) under the base case scenario and half load operating conditions. The basic calculation steps of the procedure with the corresponding parameters values for Loc1 at full load simulation are shown in Table 3.

Table 3: Loc1 full load simulation calculation steps

	Symbol	*Unit*	*Value*	*Comment*
Fatigue Damage	A	-	81.94	From FV566 LCF tests
	C	-	0.3288	For FV566 LCF tests
	D	-	1.64	For FV566 LCF tests
	$\Delta\bar{\varepsilon}_{\mathrm{t\,max}}$ max value of $\bar{\varepsilon}(t,t')$	-	0.0066	From FE analysis
Creep Damage	E	MPa	210580	Calculated at the temperature of the considered location
	$\Delta\sigma'$	MPa	115	From FE analysis
	ε_c	-	0.0000075	From FE analysis
	Z	-	0.0137	From equation in Figure 4
	ε_L	-	0.10	From [21]

The calculated damage values and the total lives of each location operating under each different loading condition are summarised in Table 4.

Table 4: Summary of the calculated damage values and total life estimations

Location	**Fatigue damage/cycle, D_f**	**Creep damage/cycle, D_c**	**Total damage, D**	**Cycles to failure**	**Failure (hr)**
		Original Load (3,000rpm)			
Loc1 (Hot region)	0.00012	0.000075	0.000195	5,128	123,077
Loc2 (Cold region)	0.000093	0.000012	0.000105	9,524	228,571
		Half Load (1,500rpm)			
Loc1 (Hot region)	0.000035	0.000073	0.000108	9,259	222,222
Loc2 (Cold region)	0.000027	0.000011	0.000038	26,316	631,579

The failure in hours is calculated from the cycles to failure considering that the duration of one cycle is 24 hours as stated in section 3.2.

Under the typical (full load, i.e. 3,000rpm) loading condition, the predicted time of failure at the high temperature location (Loc1) is estimated at 123,077 hours while for the cold location (Loc2) the time of failure is estimated at 228,571 hours. The result shows a good agreement with the typical lifetime of an industrial gas turbine rotor which lies between 100,000 - 150,000 hours of operation. From the damage values of Table 2, it is clearly observed that fatigue damage dominates the cold region whereas the effect of creep-fatigue interaction becomes present in the high temperature region. A considerable increase in the life prediction for both locations is observed when the operating load is reduced to 1,500rpm. Although, the predicted lifetime shows a significant increase, as expected, it is believed that the results are still under-estimated. This is due to the identical temperature profile used in the half load simulation. In reality, the temperature of operation in a gas turbine application should be directly proportional to its loading state. In general, the calculated life of the gas turbine rotor operating under the typical loading

condition shows a good agreement with the expected lifetime of a typical gas turbine which is attributed to the ability of the procedure to capture accurate results.

4. Conclusions and Future Work

More accurate methods to estimate the life of structures operating under thermomechanical loading will be of paramount importance in the future. This paper presents a novel integrated lifing approach using a viscoplasticity based framework due to its ability to reproduce the material behaviour under cyclic loading conditions. Using the viscoplasticity model allows the user to extract important information directly, such as stress relaxation per cycle and the elastic follow-up factor which are required to conduct a R5 life assessment procedure. This in result, significantly simplifies the R5 procedure, subsequently making the approach more attractive to be used at industrial level. The damage values obtained, show that fatigue dominates the damage process in cold regions whereas the effect of creep-fatigue interaction becomes more significant in high temperature regions. This indicates that temperature dominates the magnitude of creep damage. The results are compared with those obtained when the load condition applied is halved. This loading configuration extends the predicted lifetime in all locations.

In general, the calculated life of the gas turbine rotor operating under the typical loading condition shows a good agreement with the expected lifetime of a typical gas turbine which is attributed to the ability of the procedure to capture accurate results.

Future research should focus on three main areas: validating the model on real-world data, comparing the damage values of the present study with those obtained when an identical simulation is modelled in 3D, and performing a complete sensitivity analysis on the influence that each parameter has on the calculated damage. The eventual and ultimate goal of this study is to demonstrate the possibility of linking a viscoplasticity modelling approach with the R5 life assessment procedure that would benefit both design engineers and industrial plant operators from the simplicity and accuracy of the approach.

Acknowledgements

This work was supported by the Engineering and Physical Sciences Research Council (Grant numbers: EP/G037345/1; EP/L016206). The funding is provided through the EPSRC Centres for Doctoral Training in Carbon Capture and Storage and Cleaner Fossil Energy (**www.ccscfe-cdt.ac.uk**) and Innovative Metal Processing (**www.impact.ac.uk**).The authors would like to thank RWE for their valuable contribution and for permission to publish this paper.

REFERENCES

[1] C. Shen, "Modeling Creep-Fatigue-Environment Interactions in Steam Turbine Rotor Materials for Advanced Ultra-supercritical Coal Power Plants,"; General Electric Global Research, Niskayuna, NY (United States)2014, Available: https://www.osti.gov/servlets/purl/1134364.

[2] R. E. Dundas, "The Use of Performance-Monitoring to Prevent Compressor and Turbine Blade Failures," in *ASME 1982 International Gas Turbine Conference and Exhibit*, 2015, vol. Volume 3: Coal, Biomass and Alternative Fuels; Combustion and Fuels; Oil and Gas Applications; Cycle Innovations.

[3] M. Chrzanowski, "Use of the damage concept in describing creep-fatigue interaction under prescribed stress," *International Journal of Mechanical Sciences,* vol. 18, no. 2, pp. 69-73, 1976.

[4] Y.-N. Fan, H.-J. Shi, and K. Tokuda, "A generalized hysteresis energy method for fatigue and creep-fatigue life prediction of 316L(N)," *Materials Science and Engineering: A,* vol. 625, 2015.

[5] S. S. Manson, "Interfaces between fatigue, creep, and fracture," *International Journal of Fracture Mechanics,* vol. 2, no. 1, pp. 327-327, 1966.

[6] R. HILL, "A VARIATIONAL PRINCIPLE OF MAXIMUM PLASTIC WORK IN CLASSICAL PLASTICITY," *The Quarterly Journal of Mechanics and Applied Mathematics,* vol. 1, no. 1, pp. 18-28, 1948.

[7] W. Prager, "The Theory of Plasticity: A Survey of Recent Achievements," *Proceedings of the Institution of Mechanical Engineers,* vol. 169, no. 1, pp. 41-57, 1955.

[8] R. W. Neu and H. Sehitoglu, "Thermomechanical fatigue, oxidation, and creep: Part i. Damage mechanisms," *Metallurgical Transactions A,* vol. 20, no. 9, pp. 1755-1767, 1989.

[9] R. W. Neu and H. Sehitoglu, "Thermomechanical fatigue, oxidation, and Creep: Part II. Life prediction," *Metallurgical Transactions A,* vol. 20, no. 9, pp. 1769-1783, September 01 1989.

[10] R. P. Skelton and M. S. Loveday, "A re-interpretation of the BCR/VAMAS low cycle fatigue intercomparison programme using an energy criterion," *Materials at High Temperatures,* vol. 14, no. 1, pp. 53-68, 1997/01/01 1997.

[11] G. Marahleh, A. R. I. Kheder, and H. F. Hamad, "Creep-life prediction of service-exposed turbine blades," *Materials Science,* vol. 42, no. 4, p. 476, 2006.

[12] J. L. Chaboche, "Constitutive equations for cyclic plasticity and cyclic viscoplasticity," *International Journal of Plasticity,* vol. 5, no. 3, pp. 247-302, 1989/01/01/ 1989.

[13] A. Benaarbia, Y. Rae, and W. Sun, "Unified viscoplasticity modelling and its application to fatigue-creep behaviour of gas turbine rotor," *International Journal of Mechanical Sciences,* vol. 136, pp. 36-49, 2018.

[14] A. Benaarbia, J. P. Rouse, and W. Sun, "A thermodynamically-based viscoelastic-viscoplastic model for the high temperature cyclic behaviour of 9–12% Cr steels," *International Journal of Plasticity,* vol. 107, pp. 100-121, 2018.

[15] A. Nayebi, H. Ranjbar, and H. Rokhgireh, "Analysis of unified continuum damage mechanics model of gas turbine rotor steel: Life assessment," *Proceedings of the Institution of Mechanical Engineers, Part L: Journal of Materials: Design and Applications,* vol. 227, no. 3, pp. 216-225, 2013.

[16] *Boiler and Pressure Vessel Code* 2010.

[17] Association française pour les règles de conception, *RCC-MR: Design and Construction Rules for Mechanical Components of Nuclear Installations*. AFCEN, 2007.

[18] R. A. Ainsworth, P. J. Budden, and R. Hales, *Assessment of the high-temperature response of structures: developments in the R5 procedure*. United Kingdom: Mechanical Engineering Publications, 1996.

[19] Y. Takahashi, "Study on Creep-Fatigue Life Prediction Methods Based on Long-Term Creep- Fatigue Tests for Austenitic Stainless Steel," Dordrecht, 2001, pp. 311-320: Springer Netherlands.
[20] C. J. Smithells, *Metals reference book*. Elsevier, 2013.
[21] Y. Rae, A. Benaarbia, J. Hughes, and W. Sun, "Experimental characterisation and computational modelling of cyclic viscoplastic behaviour of turbine steel," *International Journal of Fatigue,* vol. 124, pp. 581-594, 2019.
[22] R. A. Barrett, P. E. O'Donoghue, and S. B. Leen, "An improved unified viscoplastic constitutive model for strain-rate sensitivity in high temperature fatigue," *International Journal of Fatigue,* vol. 48, pp. 192-204, 2013.
[23] S. T. Kyaw, J. P. Rouse, J. Lu, and W. Sun, "Determination of material parameters for a unified viscoplasticity-damage model for a P91 power plant steel," *International Journal of Mechanical Sciences,* vol. 115-116, pp. 168-179, 2016.
[24] J. Lu, W. Sun, A. Becker, and A. A. Saad, "Simulation of the fatigue behaviour of a power plant steel with a damage variable," *International Journal of Mechanical Sciences,* vol. 100, pp. 145-157, 2015.
[25] W. Sun, D. W. J. Tanner, T. H. Hyde, and A. A. Saad, "Thermal-mechanical fatigue behaviour of 9–12%Cr power plant steels and pipes," in *International Conference on Sustainable Power Generation and Supply (SUPERGEN 2012)*, 2012, pp. 1-8.
[26] Y. Rae, X. Guo, A. Benaarbia, N. Neate, and W. Sun, "On the microstructural evolution in 12% Cr turbine steel during low cycle fatigue at elevated temperature," *Materials Science and Engineering: A,* vol. 773, p. 138864, 2020.

Conflict of Interest and Authorship Conformation Form

Please check the following as appropriate:

- o All authors have participated in (a) conception and design, or analysis and interpretation of the data; (b) drafting the article or revising it critically for important intellectual content; and (c) approval of the final version.

- o This manuscript has not been submitted to, nor is under review at, another journal or other publishing venue.

- o The authors have no affiliation with any organization with a direct or indirect financial interest in the subject matter discussed in the manuscript

- o The following authors have affiliations with organizations with direct or indirect financial interest in the subject matter discussed in the manuscript:

Author's name	Affiliation